Defence Science Journal, Vol. 72, No. 6, November 2022, pp. 783-792, DOI : 10.14429/dsj.72.18369

Optimal Design of Hydraulic Disc Brake for Magnetorheological (MR) Application

Danishtah Quamar and Chiranjit Sarkar*

Indian Institute of Technology Patna, Bihta, Bihar – 801 106, India
**E-mail: csarkar@iitp.ac.in*

ABSTRACT

This paper aims to provide a new design considering compressive force application in the MR fluid and improve its braking torque by optimizing it. According to the current study, compressing the MR region will increase braking torque compared to no compression. The area covered by an existing model of the conventional disc brake is taken into consideration for the unique design of the MR brake to operate in shear and compression mode, and the required compression given by the hydraulic pressure similar to a conventional disc brake. The suggested MR brake's structural layout is presented. The Herschel-Bulkley shear thinning model's mathematical expression for the torque equation for the compression and shear modes is provided. An analytical magnetic circuit is done for the proposed design for determining the relationship between applied current and magnetic field strength as a function of the geometrical and material attributes of the MR brake. Simulation is done on COMSOL software with the help of an AC/DC module, considering the non-linear relationship between the magnetic field and magnetic flux. Simulation results of braking torque achieved with the varying current are determined. The graph displays the braking torque for current in the compression plus shear mode as well as shear mode. After that, optimization is done on the proposed model for optimal design parameters. For optimization, we adopt the most popular Genetic Algorithm (GA) method. Optimization aims to increase the braking torque capacity of the MR brake for the given volume.

Keywords: Magnetorheological brake; Magnetorheological fluid; Hydraulic pressure; Herschel-Bulkley model; Compression plus shear mode; COMSOL; Optimization; Genetic Algorithm (GA); Braking torque

1. INTRODUCTION

Vehicle safety primarily depends on the braking system as a sound braking system allows the vehicle to stop safely and provides a comfortable ride. So, the brake is a vital device in the vehicle system. The automotive industry is researching braking systems for safe driving. Researchers are focussing on improving braking torque efficiency and also reducing weight. To enhance the efficiency of a braking system, the active trend is to replace the conventional disc brake with the Magnetorheological (MR) disc brake because of its negligible wear effect, fast response, and excellent reliability. Conventional brake wears with time because of friction, deteriorating the brake efficiency[1]. Since the MR brake's friction performance is time-invariant, it can be used to replace disc brakes.[2-3] Devices based on MR have applications in braking, clutch, dampers, and valves.[4-5] Smart material MR fluid can be utilized as brake friction material.[6-7] Because adopting MR brakes requires less braking torque, the research initially concentrated on the design, control, and assessment of prosthetic devices.[8-13]

The ideal MR brake design has been studied by Karakoc, *et al*. considering multi-disc configuration and getting the optimal design parameter with the help of a simulated annealing algorithm.[14] Park, *et al*. have studied mass and torque-based interdisciplinary optimization of vehicle MR brakes.[15] Nguyen, *et al*. looked at the best MR brake design for a mid-sized car, considering the space available, braking torque, weight, and steady temperature produced by the MR brake operating at a zero-field friction torque when going at 100 km/h.[3] The optimum analysis of motorcycle MR brakes was carried out by Nguyen, *et al.*, who took into account the braking torque, mass, frictional temperature, and geometric dimensions.[16]

At first, the study of MR brake's yield stress was due to the shear phenomenon of MR fluids.[1-3,17-19] According to Tang, *et al*., squeezing the MR fluid in the direction of the magnetic field increases the yield shear stress to a high value.[20] Additionally, according to Tao, *et al.*, the operation of compression aggregation at the endpoints of the MR chain boosts the fluid's yield strength.[21] There is considerable research considering the compression of MR fluid for calculating the yield stress and getting a more significant value than the shear phenomenon of MR fluid.[22-26] Generally, we use the field-dependent Bingham rheological model and the Herschel-Bulkley rheological model for the torque analysis of MR brake. Nguyen, *et al*. and Farjoud, *et al.* have shown that the analytical braking torque has not provided satisfactory results.[3,27] Hence Herschel-Bulkley model is used for the torque analysis. Nguyen, *et al.*, Sarkar, *et al.*, Shamieh, *et al.*, and many other researchers have done torque analysis with the Herschel-Bulkley model.[3,26,28]

Based on the above review, this work's main contribution is to develop a novel configuration of MR brake that can substitute the standard disc brake. The proposed design utilises both the MR fluid's shear and compression modes to get the required braking torque. The mathematical expression of braking torque

Received : 4 August 2022, Revised : 27 October 2022
Accepted : 3 November 2022, Online published : 6 December 2022

is obtained by considering the Herschel-Bulkley model, and the optimal design of the MR brake is regarded with a significant focus on geometry. The important geometric dimensions and necessary braking torque are, respectively, considered design restrictions and objective functions in the optimization process. When trying to maximize or decrease the value of an objective function under a certain set of constraints, genetic algorithms are most frequently used. Biologically inspired operators like mutation, crossover, and selection are employed in genetic algorithms to produce high-quality solutions to optimization and search problems. By using the genetic algorithm, the best solutions are obtained.

2. HYDRAULIC DISC MR BRAKE

This study proposes a novel design for the MR brake to replace the traditional disc brake. A new hydraulic disc MR brake was designed, as indicated in Fig. 1, taking into account the available space for the traditional brake. The available dimensions of conventional disc brake and the suggested MR brake with its significant geometrical parameters are depicted in Table 1 and 2, respectively. The planned MR Brake is depicted as having a single rotating disc and immovable housing plates (covering the central electromagnet). The annular space surrounding and on each side of the disc, which is positioned on the shaft, is filled with MR fluid. When the piston is under hydraulic pressure, the wiper seals allow sliding while sealing the MR fluid. To impede the force generated by the hydraulic action, eight extension springs are employed. 326 turns of AWG 24 copper wire make up the central electromagnet. The number of turns is taken as 326, which is given according to the formula:

$$N_c \times A_w = 0.8 \times A_R$$

where N_c = number of turns
A_w = cross-section area of wire = 0.2 mm^2
A_r = cross-section area of core

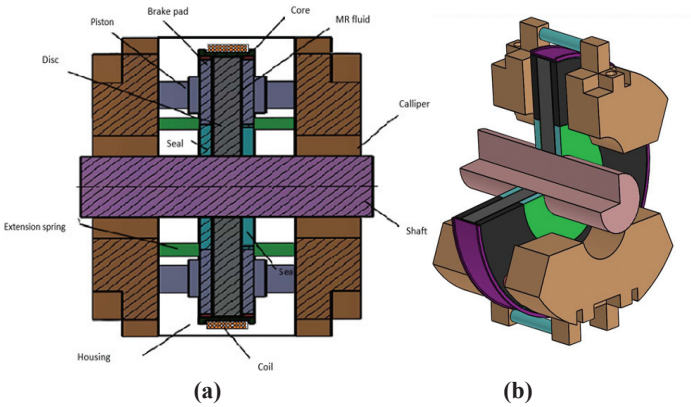

Figure 1. (a) 2D schematic illustration of proposed MR brake, and (b) 3D schematic illustration of the proposed MR brake.

3. MATHEMATICAL MODELING OF THE MR BRAKE

The main challenge in the design of MR brakes is to develop the relation between braking torque, geometric dimensions, and magnetic field intensity. As a result, a model of the suggested MR brake using Computer-Aided Design (CAD) is created using SolidWorks to calculate the torque equation, as seen in Fig. 1. Similar to Sarkar, *et al*., the suggested system applies braking torque through shear plus compression[26]. Sarkar, *et al*. study would be a basis for deriving the torque equations for the proposed system considering both shear and compression mode[26]. When calculating the braking torque, the active region and inactive zone are taken into account. When MR fluid and an applied magnetic field interact, the active region is defined, and when MR fluid is unaffected by the magnetic field, the inactive region is defined. In this study, only active regions are considered for calculating braking torque.

Table 1. Available dimensions of conventional disc brake

Components	Dimensions(mm)
Caliper	Radial thickness = 175.5, Thickness = 55
Piston	Piston dia.= 40, Connecting rod dia.= 30, Thickness of piston = 10, Thickness of Connecting rod = 10
Brake pad	Thickness = 10, Length = 80
Disc	Inner radius = 34, Outer radius = 144, Thickness = 23

Table 2 Dimensions of proposed hydraulic MR brake

Components	Dimensions(mm)
Caliper	Radial length = 165.5, Thickness = 55
Piston	Piston dia.= 40, Connecting rod dia.= 30, Thickness of piston = 10, Thickness of connecting rod = 10
Brake pad	Inner radius = 69, Outer radius = 144, Thickness = 10
Disc	Inner radius = 34, Outer radius = 144, Thickness = 23
Core	Thickness = 2.5
Coil	Area = 40.2*2.027
Housing	Above the core = 16.473
Extension spring	Length = 15, Outer dia.= 14
MRF gap b/w brake pad and disc	1 (in case of shear), 0.5 (in case of compression)
MRF gap b/w core and disc	0.5
Seal b/w core and brake pad	Length = 0.5, Thickness = 10
Seal b/w brake pad and shaft	Length = 35, Thickness = 10
Shaft	Radius = 34

The shear stress that occurred in the MR fluid acting just in shear mode can be represented as follows using the model of Herschel-Bulkley:

$$\tau = \tau_{yd}(H) + K\dot{\gamma}^{n} \quad (1)$$

Here the first term is yield strength which depends on the applied field intensity H. K and n are the zero-field consistency and flow behavior index, and the $\dot{\gamma}$ is the MR fluid's shear strain rate, which is roughly represented by,

$$\dot{\gamma} = \frac{r \times \omega}{h} \quad (2)$$

where h is the MR fluid gap, ω is the shaft's angular velocity, and r is the disc's radial distance.

The consistency and flow behavior index is represented by the parameters K and n respectively. Both are fluid properties, and it varies on applied magnetic-flux density. According to Zubieta, *et al*., the relation between the rheological characteristics that vary with field and the magnetic flux B is given as[29]:

$$K = K_{\infty} + (K_o - K_{\infty})(2e^{-B\alpha_{SK}} - e^{-2B\alpha_{SK}}) \quad (3)$$

$$n = n_{\infty} + (n_o - n_{\infty})(2e^{-B\alpha_{Sn}} - e^{-2B\alpha_{Sn}}) \quad (4)$$

$$\tau_y = \tau_{y\infty} + (\tau_{yo} - \tau_{y\infty})(2e^{-B\alpha_{STy}} - e^{-2B\alpha_{STy}}) \quad (5)$$

K_o, n_o, τ_{y_o} are the properties at zero magnetic fields, and $K_{\infty}, n_{\infty}, \tau_{y_{\infty}}$ are the properties at saturation value. α_{SK}, α_{Sn}, and α_{ST_y} are related to torque.

Tao, *et al.* have modelled the MR fluid's yield shear stress under compression:[20]

$$\tau_y(H) = \tau_{yd}(H) + K(H)P_e \quad (6)$$

The first term is the MR fluid's yield shear stress when there is no compression, and the subsequent term indicates the linear correlation between shear stress and compression pressure (P_e). K(H) is calculated by performing experiments on a magneto rheometer and found that it is independent of pressure and magnetic field intensity, but K(H) may depend on H based on electromagnetic force.[26]

Hence, the Herschel-Bulkley MR fluid model under compression is given by putting Eqn. (6) into Eqn. (1):

$$\tau_c = \tau_{yd}(H) + K(H)P_e + K\dot{\gamma}^{n} \quad (7)$$

Hence, the transmitted torque in the MR brake on one side of the rotating disc is given as:

$$\text{(a) } dT = 2\pi\tau r^2 dr(\text{for\_shear})$$

$$\text{(b) } dT = 2\pi\tau_c r^2 dr(\text{for\_compression}) \quad (8)$$

Integrating Eqn. (8) from r_i to r_o and multiplying it by 2 gives the torque transmitted on both sides of the rotating disc, where r_i is the lower limit of the disc and r_o is the upper limit of the disc.

For the shear mode of operation, transmitted torque given as:[26]

$$T_b = \frac{4\pi}{3}(r_2^3 - r_1^3)\tau_{yd}(H) + \frac{4\pi K\omega^n}{(n+3)h_c^n}(r_2^{n+3} - r_1^{n+3}) \quad (9)$$

For the compression mode of operation, transmitted torque given as:[26]

$$T_b = \frac{4\pi}{3}(r_2^3 - r_1^3)(\tau_{yd}(H) + K(H)P_e) + \frac{4\pi K\omega^n}{(n+3)h_c^n}(r_2^{n+3} - r_1^{n+3}) \quad (10)$$

Eqn. (9) and Eqn. (10) give the required braking torque under shear and compression mode of operation, respectively, on both rotor surfaces in the active zone. Here the torque created by the applied field is the first term and the second term is the torque produced by the MR fluid's viscous friction in the active zone. The MR fluid's viscous friction in the inactive area is assumed to be negligible while considering the torque equation.

4. ANALYTICAL MAGNETOSTATIC CIRCUIT ANALYSIS

To get the connection between MR fluid's applied current and magnetic field strength, the magneto-rheological brake's magnetic circuit has to be analyzed. In the proposed brake, after applying hydraulic pressure, the coil current has to increase for achieving the necessary yield stress after activating the core electromagnet. The magnetic circuit of the proposed work is shown in a 2D axisymmetric design made in COMSOL software to reduce the computational time during the simulation, as shown in Fig. 2. The shear mode and compression mode generate the same magnetic circuit; the only difference is that the MR fluid gap gets lesser over compression. Figure 3 illustrates the suggested MR brake's dimensions.

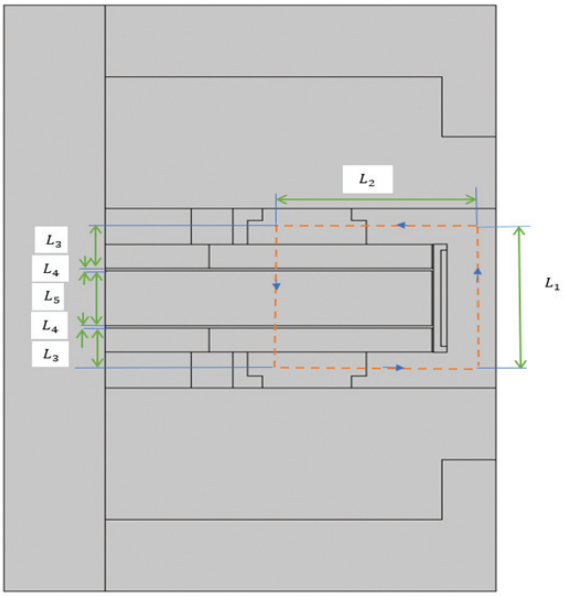

Figure 2. Magnetic circuit under operation.

The entire magnetic circuit of the proposed MR brake is divided into five parts, as shown in Fig. 2. For a magnetic circuit, the relationship between the current and the effective length of each piece and the magnetic field intensity of various sections may be found using Ampere's Law as per Shamieh, *et al.*[28]:

$$\sum H_k \times L_k = N_c \times I \tag{11}$$

where N_c is the coil's number of turns, (I) is the applied current, and the strength of the magnetic field and a reasonable length for the circuit's k_{th} link are denoted by H_k and L_k, respectively. Now, according to Shamieh, *et al*., since the magnetic flux is conserved, the circuit's description of its continuity is:[28]

$$\phi = B_k \times A_k \tag{12}$$

where the magnetic flux is ϕ , the k_{th} link's cross-sectional area is A_k, and the magnetic flux density is B_k which is described by

$$B_k = \mu_{fs} \times \mu_k \times H_k \tag{13}$$

$\mu_{fs} = 4\pi * 10^{-7}\ \mathrm{Tm\,A^{-1}}$ is the free space's magnetic permeability, and μ_k is the k_{th} link's relative permeability.

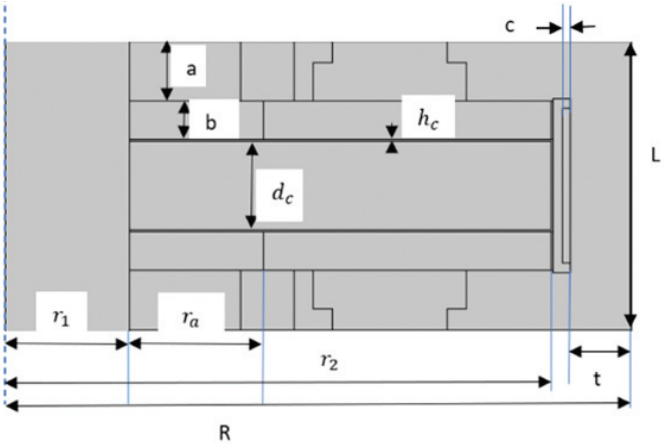

Figure 3. Geometric dimensions of proposed MR brake.

The analysis of the magnetic circuit was carried out under the assumption that the magnetic field was uniform and the constant relative permeability. But the magnetic field intensity is not uniform in the MR fluid region.

The effective length of the links of the magnetic circuit and their corresponding cross-sectional area, as shown in Fig. 2, is considered following Shamieh, *et al*.:[28]

$$L_1 = L - (a + b) \tag{14}$$

$$L_2 = R - \frac{r_2 + r_1 + r_a + t}{2} \tag{15}$$

$$L_3 = \frac{a + b}{2} \tag{16}$$

$$L_4 = h_c \tag{17}$$

$$L_5 = d_c \tag{18}$$

$$A_1 = \pi[R^2 - (R - t)^2] \tag{19}$$

$$A_2 = \pi(a + b)(R - t + r_1 + r_a) \tag{20}$$

$$A_3 = A_4 = A_5 = \pi[r_2^2 - (r_1 + r_a)^2] \tag{21}$$

In the proposed MR brake design the metal component is silicon steel. So, considering Eqn. (11) and Fig. 2, it is written as:

$$N_c \times I = (L_1 + 2L_2 + 2L_3 + L_5)H_s + 2L_4 H_f \tag{22}$$

H_s and H_f are the magnetic field of silicon steel and MR fluid links, respectively. Now, using Eqn. (12) and (13), it can be written as:

$$H_s = \frac{\phi}{\mu_{fs} \times \mu_s \times A_s} = \frac{B_f \times A_f}{\mu_{fs} \times \mu_s \times A_s} \tag{23}$$

Eqn. (13) can be put into Eqn. (23) to determine the correlation between MR fluid and silicon steel's magnetic field. This relationship is expressed as follows:

$$H_s = \left(\frac{\mu_f \times A_f}{\mu_s \times A_s}\right) H_f \tag{24}$$

s and f subscript are for silicon steel and MR fluid, respectively.

Although it may change with the strength of the magnetic field, the computation will treat the relative permeability of the MR fluid and metallic component as constant[27]. Finally, the magnetic field in the area of MR fluid can be estimated by replacing Eqn. (24) with Eqn. (22).

$$H_f = \frac{N_c \times I}{\left(\frac{\mu_f}{\mu_s}\right)\left(L_1 \frac{A_3}{A_1} + 2L_2 \frac{A_3}{A_2} + 2L_3 + L_5\right) + L_4} \tag{25}$$

5. SIMULATION OF THE MR BRAKE

The current research analyses the magnetic circuit produced in the proposed MR brake using the commercial FEM tool COMSOL Multiphysics by adding AC/DC module. Simulation has been carried out in simulation software Comsol Multiphysics 5.3a software to determine the yield stress dependence on the magnetic field. Many simulation works have been done over Comsol Multiphysics software for magnetic field simulation.[30-32,37] In the MR brake domain, it is utilized to compute the magnetic field and its distributions. Maxwell's equations are solved using magnetic vector potential in simulation software for each domain. The rectangular shape around the MR brake acts as a magnetic insulator represented by air. As MRF-132DG has a more significant operating temperature, it is used in the current study.

The non-linear magnetic properties (BH curve), yield stress vs magnetic field of MR fluid 132DG are given by Lord Corporation.[33] The different materials used in the proposed MR brake design are shown in Table 3. The non-linear magnetic properties (BH curve) for the magnetic materials are considered from the COMSOL material library. For modeling the multiturn coil, copper material is used. For generating the magnetic field in the proposed model, Ampere's Law is used, and the non-linear HB curve is used as the constitutive relation for the MR fluid and the silicon steel. A simulation study was done on the stationary solver considering varying current over parametric sweep in which the current value is taken as 0A, 1A, 2A, 3A, and 4A. For getting the braking torque, the line

integration is done on each active MRF zone with the help of the post-processor of the AC/DC module.

Table 3. Material and relative permeability of MR brake components

Components	Materials	Relative Permeability
Shaft	Aluminum	1
Caliper	Aluminum	1
Piston	Silicon Steel	H-B curve
Spring	Aluminum	1
Core	Aluminum	1
Coil	Copper	-
Wiper Seal	Natural Rubber	1
Brake pad	Silicon Steel	H-B curve
Disc	Silicon Steel	H-B curve
MR fluid	MRF-132DG	H-B curve
Housing below piston	Aluminum	1
Housing above piston	Silicon Steel	H-B curve

6. DESIGN OPTIMIZATION

In this section, following the magnetostatic analysis, the optimal design problem considering the maximization of total braking torque is taken for the compression mode of operation. As per the literature, there is an MR brake with compression application on the MR fluid in which the braking torque is 100 N-m after providing the compression on the MR fluid with the help of a side electromagnet.[26] So, to obtain the ideal design parameter, our work's purpose of optimization is to boost braking torque when the current is not zero and decrease it when the current is zero. During optimization, it is expected for braking torque to be not less than 100 N-m and magnetic flux to be not more than 250 kA/m considering Sarkar, *et al*.,[26] Besides, several design constraints must be assured for the MR brake to be successfully developed. Figure 3 depicts the suggested design's configuration together with all relevant geometric measurements. The design variables are considered which we can change for the accommodation of the proposed MR brake design in the available volume of braking system used in the most popular passenger car. The design variables (DVs), as displayed in the illustration, include coil height c, the radial distance between the core and outer boundary of MR brake t, the gap between caliper and brake pad a, the thickness of brake pad b, MR fluid gap after compression h_c, disc thickness d_c, the inner and outer diameter of disc r_1 and r_2 respectively and the seal height between the shaft and brake pad r_a. The other dimensions are fixed for feasibility. All the design variables are considered by taking care that the axial length L of the MR brake is not more than 60 mm and radial length R is not more than 200 mm. While considering the axial and radial length, the caliper dimensions are not considered for ease of calculation. The axial length is considered by the available dimension of the conventional disc brake provided in Table 1 which is 53 mm. So, for the constraint, we have considered that the axial length should not be more than 60 mm. The radial length is given according to the most popular passenger car wheel diameter.[34] The MR brake optimization problem is represented by:

*Maximize: T_b (Total braking torque)

where, $T_b = T_{on} - T_{off}$

T_{on} = the braking torque in the ON state ($I \neq 0$)
T_{off} = the braking torque in the OFF state ($I = 0$)

*subject to $T_{on} \geq 100$ N-m
$H \leq 250$ kA/m
$L \leq 60$ mm
$R \leq 200$ mm

$$\min DV_i \leq DV_i \leq \max DV_i \quad i = 1-9$$

where, $\min DV = [c_{min}\ t_{min}\ a_{min}\ b_{min}\ h_{c_{min}}\ d_{c_{min}}\ r_{2_{min}}\ r_{1_{min}}\ r_{a_{min}}]$

$$\max DV = [c_{max}\ t_{max}\ a_{max}\ b_{max}\ h_{c_{max}}\ d_{c_{max}}\ r_{2_{max}}\ r_{1_{max}}\ r_{a_{max}}]$$

A metaheuristic method called the genetic algorithm (GA) is used to solve constrained and unconstrained optimization problems. A lot of emphases has recently been paid to using GA to tackle multi-objective optimization issues where multiple criteria must be considered at once.[28,35-37]

The optimization algorithm for this work was carried out in MATLAB software. The GA solver is used from the optimization toolbox available in MATLAB R2018a. 200 population size is considered from the menu for running the solver. The lower and upper bounds of the design variables are given in Table 4. The bounds are regarded according to the available dimensions of the disc and provide the approximate assumptions for upper and lower bounds regarding available sizes for other variables.

Table 4. Lower and upper bound of the design variable

DV	DV_{min} mm	DV_{min} mm
c	2.5	96
t	1	5
a	10	21
b	8	12
h_c	0.5	1
d_c	10	20
r_2	40	120
r_1	30	38
r_a	1	3

7. RESULTS AND DISCUSSION

7.1 Magnetic Field Analysis

On computing over FEM software, the magnetic field intensity and magnetic flux density will be plotted on a 2D plot group. First, the study is performed for the proposed design without providing compression, i.e., under shear mode only. According to Mazlan, *et al*.,[24] the performance of MR fluid in compression mode has been studied where the gap before compression was taken 1mm. From there the concept has

been taken to consider the gap in shear mode (i.e; before compression) as 1 mm and after compression, it has been assumed that the gap reduces by 0.5 mm for the getting the effect of the magnetic field in shear and compression mode respectively for the finite element study of the application of MR fluid over MR brake. The plots of magnetic flux and the torque vs current graph for both shear mode and compression mode are considered and compared. The 2D plot group for the magnetic flux density for the brake under shear mode and compression mode at similarly applied current are shown in Fig. 4 and Fig. 5.

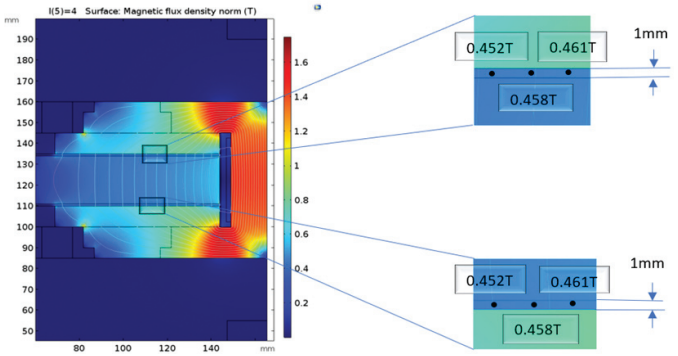

Figure 4. Magnetic flux density under shear mode at I = 4A.

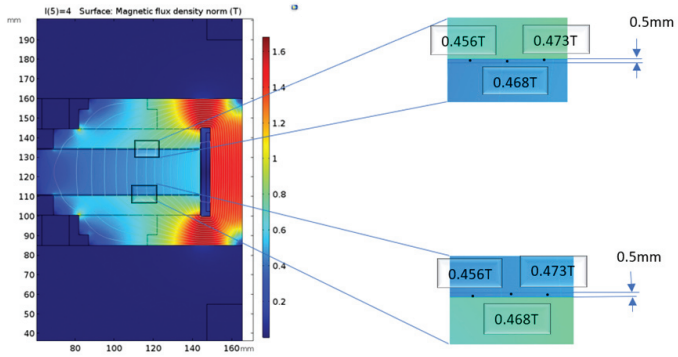

Figure 5. Magnetic flux density under compression mode at I = 4A.

Comparing Fig. 4 and Fig. 5 shows that the magnetic flux has a slightly large value on the compression of MR fluid in the active zone than that before compression. The compression of MR fluid in the direction of the magnetic field significantly improves the yield shear stress,[20] resulting in improved braking performance as there are weak points of MR microstructure at the ends of the MR chain under shear action, which results in lower yield shear stress.[21] This can be shown by plotting the current vs Braking torque graph for the shear mode and compression mode of MR fluid for the working of the MR brake.

Figures 6 and 7 show that the magnetic flux increases in the radial direction in MR fluid and has a maximum value near the coil. At every applied current, the significant rise in magnetic flux in the radial direction of MR fluid is shown in compression mode. Still, in shear mode, the growth rate is relatively slow, suggesting the magnetic flux saturation in shear mode at a lower value than in compression mode. From this, it can be concluded that the MR fluid gap plays a role in the early magnetic flux saturation. For higher MR fluid gap in the active region brings early saturation. To improve the braking performance, magnetic flux density also has to be increased, which can be obtained by giving less MR fluid gap and compressing the MR fluid. Hence the compression of fluid helps improve braking performance in two ways, one by reducing the gap and another by giving a strong bond of MR microstructure at the ends of the MR chain, as Tao, *et al.*[21] Figure 8 shows the MR microstructure before and after the magnetic field region compression.

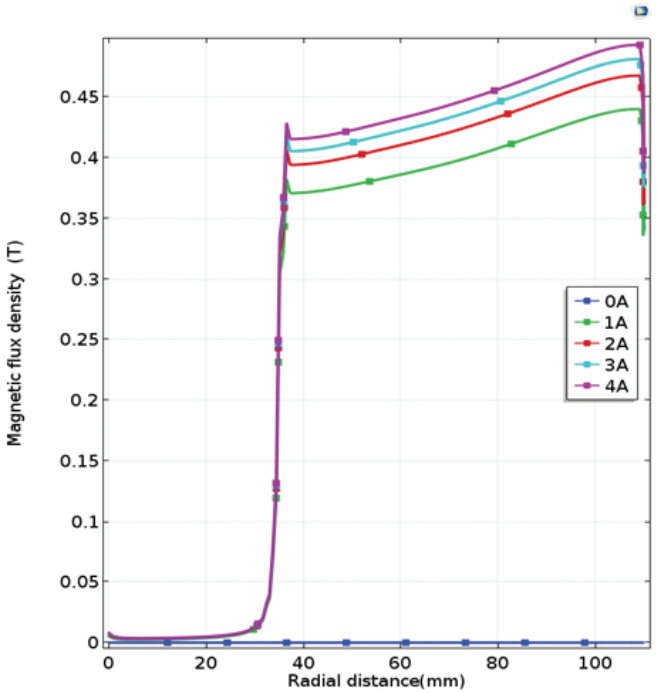

Figure 6. Magnetic flux at both MR gaps in shear mode.

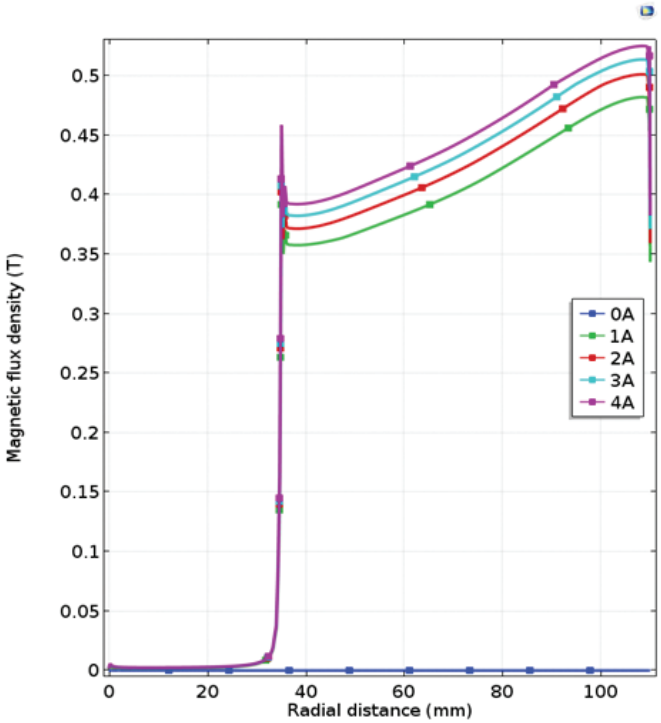

Figure 7. Magnetic flux at both MR gaps in compression mode.

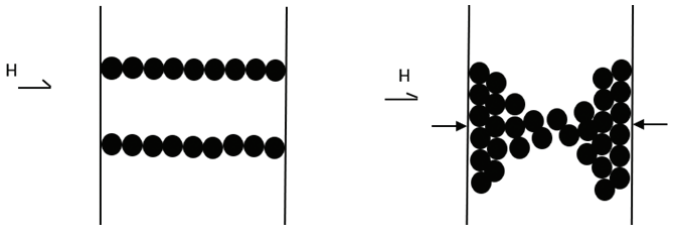

Figure 8. Formation of robust MR microstructure during compression: (a) Chains before compression, and (b) Chains aggregate into thick columns with robust ends after compression.

In Figure 9, the braking torque value has been plotted for different applied currents in both shear and compression modes. As observed in Fig. 9, the yield shear stress increases due to compression in the magnetic field direction, making the braking torque in compression mode more important for every current value than in shear mode. Also, the MR fluid gap decreases due to compression, resulting in increased magnetic flux density. It can be seen that there is a significant rise in braking torque on increasing current in the compression mode of working of the proposed design. In contrast, in shear mode, the increase of the amplitude of braking torque on improving current is relatively low due to the saturation of magnetic flux. While doing the finite element analysis over shear mode and compression mode, the rotor's RPM is taken constant and equal to 100 RPM. The pressure in compression mode is taken 6 bar for study as in hydraulic brake system, vehicle stop by regulating the pressure between 20 and 120 pounds.[38]

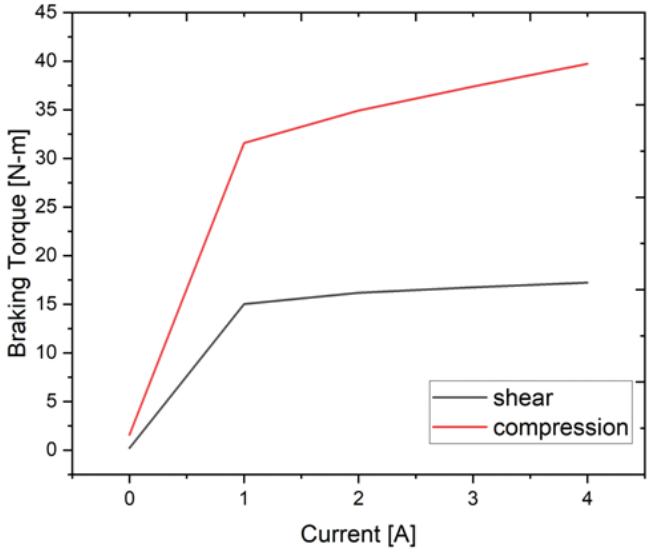

Figure 9. Braking torque under shear and compression.

As the compression mode of operation gives relatively greater braking torque than the shear mode, the compression study is done over various RPMs of the rotor, and the braking torque in compression mode at different RPMs is plotted as shown in Fig. 10.

It can be seen that there is a rise in the braking torque on increasing the RPM of the rotating disc, but the rise is significantly less because of the slight increase in the viscous torque on increasing the RPM of the rotating disc. The torque due to the magnetic field is unaffected by the rotor's RPM.

Figure 10 shows the graph between the viscous torque and the RPM of the rotating disc, the secondary X and Y-axis in red.

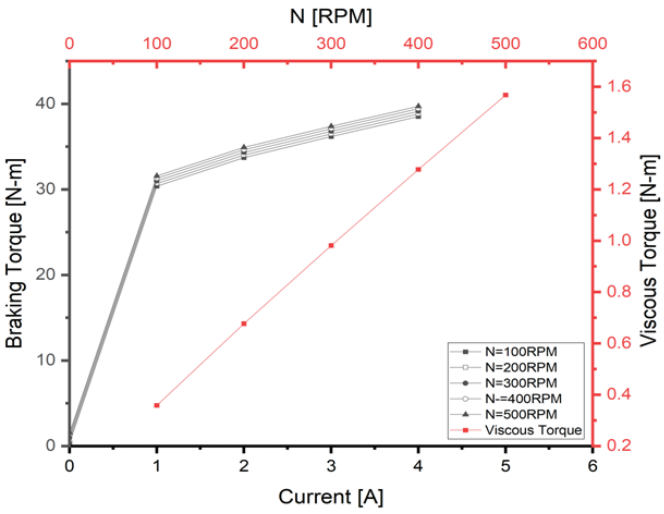

Figure 10. Braking torque and viscous torque at various RPM.

7.2 Optimal Design Analysis

For the cost function f(x), GA arrived at the lowest value of 0.008648, where the cost function is (1/Tb), in just six generations. Table 5 displays the ideal design variables that were produced and table 6 displays the performance requirements of the derived ideal MR brake design. For optimal design parameters, the current and RPM values are I=2A and N=100 RPM. The results show that the majority of the design variables remained close to their initial levels. Few geometric variables such as c, a, h_c, and r_2 witnessed the change, allowing the objective value to decrease.

Table 5. Optimum design variable using GA for the MRB

Design variables	Optimized value (mm)
c	3
t	1
a	16
b	8
h_c	1
d_c	10
r_2	120
r_1	30
r_a	1

Table 6. Specifications for the selected optimal MRB design

T_{on}	185.222 N-m
H	67.7 kA/m
L	60 mm
R	127 mm

GA code for this model gives a reasonably good result for the study by Shamieh, *et al*., in which to increase the dynamic range and reduce the response time and weight of the MRB while taking into account weight, size, and magnetic flux density limits, a multidisciplinary design optimization problem is used to discover the ideal brake geometry parameters[28]. The result calculated analytically with the obtained optimized

design parameter gives the same result as the algorithm result. The bar graph in Fig. 11(a) shows the compared design variable

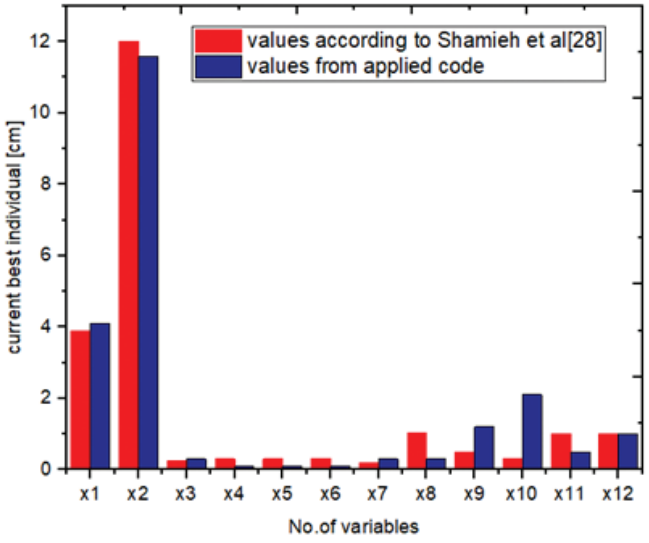

(a)

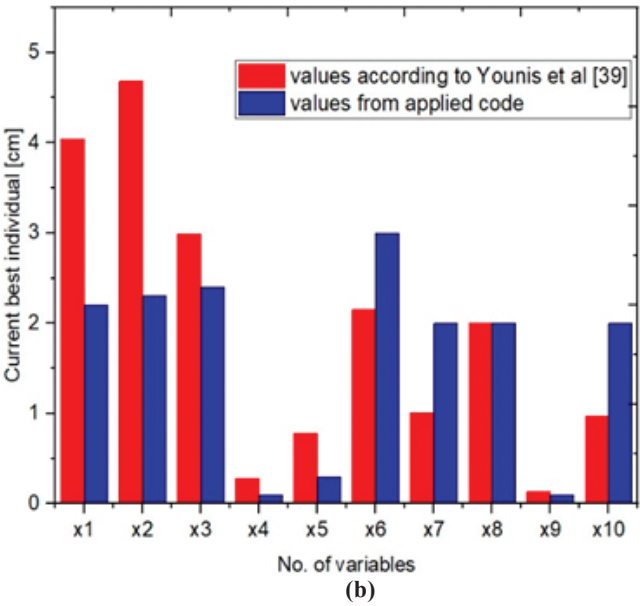

(b)

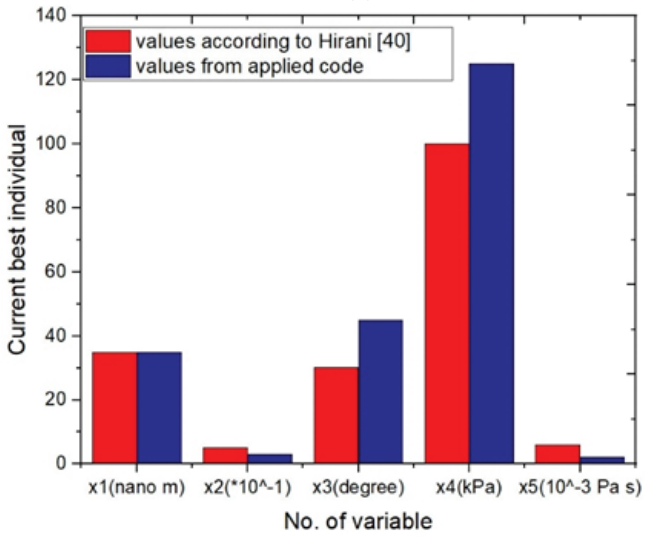

(c)

Figure 11. Comparison of literature result with the generated code.

from Shamieh[28], *et al*. and the obtained design variable from the GA code. The validation of code is also done for Younis,[39] *et al.* and Hirani[40] and the compared bar graph of the design variable has been plotted in Fig. 11(b) and 11(c) respectively.

The braking torque calculated by $T_b = T_{on} - T_{off}$ is obtained as 115.74 N-m, which is more prominent than the Sarkar,[26] *et al*. Here T_{on} is considered as braking torque in on state ($I \neq 0$) and T_{off} as braking torque in off state ($I = 0$). While doing optimization, the gap between the core and disc is considered constant and equal to 0.5 mm. The core thickness is considered stable and equal to 2.5 mm per feasibility.

8. CONCLUSIONS

The new design of the MR brake has been proposed considering the conventional disc brake design. The proposed MR brake worked under compression mode, and required compression is provided with the help of hydraulic pressure as in a traditional disc brake. The detailed Solid Work design of the proposed MR brake both in 2D and 3D is presented in this paper. The dimensions of every component of the available conventional hydraulic disc brake and proposed hydraulic MR brake are shown with the help of tables. The proposed model's analytical magnetostatic analysis and braking torque equation have been discussed. Finite element analysis is done for both shear mode, and compression mode on COMSOL software using AC/DC module, and the braking torque is calculated. On doing finite element analysis for both shear and compression modes of operation, it is found that in the shear mode of operation, there is early magnetic saturation than in the compression mode of operation. Due to an increase in yield stress during compression, the braking torque has also increased when the compression mode of operation is used. A graph is used to compare the braking torque in both the shear and compression modes, and it discusses the relationship between the braking torque and the disc's rotational speed (RPM). On increasing the RPM of rotor braking, torque rises because of the slight increase in the viscous torque with RPM, and the torque due to the magnetic field remains the same. Following finite element analysis, optimization is carried out for the optimal design parameter by increasing the braking torque in the ON state and decreasing it in the OFF state. While optimizing, constraints are put over the magnetic field, braking torque, radial length, and axial length of the MR brake. The range of design variables is set according to the feasibility of the proposed design. MATLAB R2018a is used for the optimization study in which the optimization solver is used for GA. The generated MATLAB codes are validated with the literature and presented in the form of comparison in this study. The design variables obtained after optimization give good braking torque in ON state (185.222 N-m), which is more significant than Sarkar,[26] *et al*., which works under compression mode on one side and shear mode on another rotor.

REFERENCES

1. Sukhwani, V.K. & Hirani, H. Design, development, and performance evaluation of high-speed magnetorheological brakes. *Proc. Inst. Mech. Eng. L: J. Mater.: Des. App.*,

2008, **222,** 73–82
doi: 10.1243/14644207JMDA120

2. Park, E.J.; Stoikove, D.; Falco, d.L.L.; & Suleman, A. A performance evaluation of an automotive magnetorheological brake design with a sliding mode controller. *Mechatronics,* 2006, **16**, 405–16
doi: 10.1016/j.mechatronics.2006.03.004
3. Nguyen, Q.H. & Choi, S.B. Optimal design of an automotive magnetorheological brake considering geometric dimensions and zero-field friction heat. *Smart Mater. Struct.*, 2010, **19**, 115024
doi: 10.1088/0964-1726/19/11/115024
4. Muhammad, A.; Yao, X.L. & Deng, Z.C. Review of magnetorheological (MR) fluids and its applications in vibration control. *J. Mar. Sci. Appl.*, 2006, **5,** 17–29
doi: 10.1007/s11804-006-0010-2
5. Wang, J. & Meng, G. Magnetorheological fluid devices: principles, characteristics, and applications in mechanical engineering. *Proc. Inst. Mech. Eng. L: J. Mater.: Des. App.*, 2001, **215,** 165–74
doi: 10.1243/1464420011545012
6. Sarkar, C. & Hirani, H. Synthesis and Characterization of Antifriction Magnetorheological Fluids for Brake. *Def. Sci. J.,* 2013, **63**, 408-41
doi: 10.14429/dsj.63.2633
7. Sarkar, C. & Hirani, H. Synthesis and Characterisation of Nano Silver Particle-based Magnetorheological Fluids for Brakes. *Def. Sci. J.,* 2015, **65,** 252-258
doi: 10.14429/dsj.65.7879
8. Herr, H. & Wilkenfeld, A. User-adaptive control of a magnetorheological prosthetic knee. *Ind. Robot,* 2003, **30,** 42–55
doi: 10.1108/01439910310457706
9. Liu, B.; Li, W.H.; Kosasih, P.B & Zhang, X.Z. Development of an MR-brake-based haptic device. *Smart Mater. Struct.*, 2006, **15,** 1960
doi: 10.1088/0964-1726/15/6/052
10. Gudmundsson, K.H.; Jonsdottir, F. & Thorsteinsson, F. A geometrical optimization of a magneto-rheological rotary brake in a prosthetic knee. *Smart Mater. Struct.,* 2010, **19,** 035023
doi:10.1088/0964-1726/19/3/035023
11. Demersseman, R.; Hafez, M.; Lemaire, S.B. & Clénet, S. Magnetorheological Brake for Haptic Rendering. *LNCS*, 2008, **5024,** 941–5
doi: 10.1007/978-3-540-69057-3_119
12. Blake, J. & Gurocak, H.B. Haptic Glove With MR Brakes for Virtual Reality. *Mechatronics*, 2009, **14,** 606-15
doi: 10.1109/TMECH.2008.2010934
13. Ye, S.C. & Williams, K.A. Torsional vibration control with an MR fluid brake. *SPIE Proc. Ser.*, 2005, **5760,** 283–92
doi: 10.1117/12.600174
14. Karakoc K 2007 *Masters Thesis* University of Victoria
15. Park, E.J.; Luz, L.F. & Suleman, A. Multidisciplinary design optimization of an automotive magnetorheological brake design. *Comput. Struct.,* 2008, **86**, 207–16 doi: 10.1016/j.compstruc.2007.01.035
16. Nguyen, Q.H. & Choi, S.B. Optimal design of a novel hybrid MR brake for motorcycles considering axial and radial magnetic flux. *Smart Mater. Struct.*, 2012, **21**, 055003
doi: 10.1088/0964-1726/21/5/055003
17. Huang, J.; Zhang, J.Q.; Yang, Y. & Wei, Y.Q. Analysis and design of a cylindrical magneto-rheological fluid brake. *J. Mater. Process. Technol.,* 2002, **129**, 559–62 doi: 10.1016/S0924-0136(02)00634-9
18. Li, W.H. & Du, H. Design and Experimental Evaluation of a Magnetorheological Brake. *Int. J. Adv. Manuf. Technol.*, 2003, **21**, 508–15
doi: 10.1007/s001700300060
19. Bydon S 2002 *Control Club Poz.* **20**
20. Tang, X.; Zhang, X. & Tao, R. Structure-enhanced yield stress of magnetorheological fluids. *Arch.Process J. Appl. Phys.*, 2000, **87,** 2634–8
doi: 10.1063/1.372229
21. Tao, R. Super-strong magnetorheological fluids. *J. Phy.: Condens. Matter*, 2001, **13,** R979-99
doi: 10.1088/0953-8984/13/50/202
22. Kulkarni, P.; Ciocanel, C.; Vierra, S.L. & Naganathan, N. Study of the Behavior of MR Fluids in Squeeze, Torsional and Valve Modes. *J. Intell. Mater. Syst. Struct.*, 2003, **14**, 99–104
doi: 10.1177%2F1045389X03014002005
23. Zhang, X.Z.; Gong, X.L.; Zhang, P.Q. & Wang, Q.M. Study on the mechanism of the squeeze-strengthen effect in magnetorheological fluids. *J. Appl. Phys.,* 2004, **96,** 2359–64
doi: 10.1063/1.1773379
24. Mazlan, S.A.; Ekreem, N.B. & Olabi, A.G. An investigation of the behavior of magnetorheological fluids in compression mode. *J. Mater. Process. Technol.*, 2008, **20I**, 780–5
doi: 10.1016/j.jmatprotec.2007.11.257
25. Hongyun, W.; Chang, B.; Junwu, K.; Chunfu, G. & Wang, X. The Mechanical Property of Magnetorheological Fluid Under Compression, Elongation, and Shearing. *J. Intell. Mater. Syst. Struct.*, 2011, **22,** 811-6
doi: 10.1177/1045389X11409605
26. Sarkar, C. & Hirani, H. Theoretical and experimental studies on a magnetorheological brake operating under compression plus shear mode. *Smart Mater. Struct.*, 2013, **22,** 115032
doi: 10.1088/0964-1726/22/11/115032
27. Farjoud, A.; Vahdati, N. & Fah, Y.F. Mathematical Model of Drum-type MR Brakes using Herschel-Bulkley Shear Model. *J. Intell. Mater. Syst. Struct.,* 2008, **19,** 565–72
doi: 10.1177/1045389X07077851
28. Shamieh, H. & Sedaghati, R. Multi-objective design optimization and control of magnetorheological fluid brakes for automotive applications. *Smart Mater. Struct.,* 2017, **26,** 125012
doi: 10.1088/1361-665X/aa9452
29. Zubieta, M.; Eceolaza, S.; Elejabarrieta, M.J. & Bou-Ali, M.M. Magnetorheological fluids: characterization and modeling of magnetization. *Smart Mater. Struct.*, 2009, **19**, 095019
doi: 10.1088/0964-1726/18/9/095019

30. Thakur, M.K & Sarkar, C. Design and testing of a conventional clutch filled with magnetorheological fluid activated by a flexible permanent magnet at low compressive load: Numerical simulation and experimental study. *J. of Tribology*, 2022, **144** 021205-1 doi: 10.1115/1.4052278
31. Thakur, M.K. & Sarkar, C. Experimental and Numerical Study of Magnetorheological Clutch with Sealing at Larger Radius. *Def. Sci. J.,* 2020, **70**(6), 575-582 doi: 10.14429/dsj.70.15778
32. Singh, A.; Thakur, M.K. & Sarkar, C. Design and development of a wedge-shaped magnetorheological clutch. *Proc. Inst. Mech. Eng. L: J. Mater.: Des. App.,* 2020, **234**(9) doi: 10.1177/1464420720931886
33. MRF-132DG Magneto-Rheological Fluid, Lord technical data
34. Patel, M.; Raval, M. & Patel, J. Design of disc brake rotor *Int. J. Eng. Res. Dev*, 2016, **4,** 2321-9939
35. Chi, Z. & Zhang, D. Multi-objective optimization of stiffness and workspace for a parallel kinematic machine. *Int. J. Mech. Mater. Des.*, 2013, **9**(3), 281–293
36. Liu, G.P.; Han, X. & Jiang, C. An efficient multi-objective optimization approach based on the micro genetic algorithm and its application. *Int. J. Mech. Mater. Des.*, 2012, 8(**1**), 37–49 doi: 10.1007/s10999-011-9174-2
37. Hajiyan, M.; Mahmud, S.; Biglarbegian, M. & Abdullah, H.A. A new design of the magnetorheological fluid-based braking system using genetic algorithm optimization. *Int J Mech Mater Des.*, 2016, **12**, 449–462 doi: 10.1007/s10999-015-9322-1
38. From pedal to pads, https://www.knowyourparts.com
39. Younis, A.; Karakoc, K.; Dong, Z.; Park, E. & Suleman, A. Application of SEUMRE global optimization algorithm in automotive magnetorheological brake design. *Struct Multidisc Optim*, 2011, **44**, 761-772 doi: 10.1007/s00158-011-0661-8
40. Hirani, H. Multiobjective optimization of journal bearing using mass conserving and genetic algorithms, Proceedings of the Institution of Mechanical Engineers, Part J: Journal of Engineering Tribology. *Proc. Inst. Mech. Eng. J: J. Tribol.,* 2005, **219**, 235-248. doi: 10.1243/135065005X9844

CONTRIBUTORS

Mrs Danishtah Quamar did her Bachelors of Technology in the Mechanical Engineering Department from Jamia Millia Islamia, New Delhi. She completed Master of Technology in Mechanical Engineering with specialization in Design, from Jamia Millia Islamia, New Delhi. Currently, she is pursuing her PhD in Mechanical Engineering Department (Design) at IIT Patna. Her research focuses on the development and optimization of the magnetorheological (MR) brake.

For the present study, she ran the simulation and made the suggested MR brake more effectively. She wrote the paper and plotted the graphs.

Dr Chiranjit Sarkar completed his Post Doctoral work at Lulea University of Technology in Sweden after earning his PhD from the Indian Institute of Technology, Delhi. He is currently working at IIT Patna's Mechanical Engineering Department as an Assistant Professor. He has one patent for the Magnetorheological Brake design and 51 research papers published in various regional, national, and worldwide journals. His scientific interests include the design of biomedical devices, tribology, CFD of grease flow, magnetorheological (MR) fluids and devices, and ergonomics in design.

He reviewed the present manuscript and recommended every simulation and optimization study that was stated in the report.